

Crystal Growth, Structure, and Electronic Band Structure of Tetracene–TCNQ

A. J. C. Buurma,[†] O. D. Jurchescu,[†] I. Shokaryev,[†] J. Baas,[†] A. Meetsma,[†] G. A. de Wijs,[‡] R. A. de Groot,^{†,‡} and T. T. M. Palstra^{*,†}

Solid State Chemistry Laboratory, Materials Science Centre, University of Groningen, Nijenborgh 4, 9747 AG Groningen, The Netherlands and Electronic Structure of Materials, University of Nijmegen, Toernooiveld 1, 6525 ED Nijmegen, The Netherlands

Received: September 12, 2006; In Final Form: December 6, 2006

We have grown the charge-transfer salt of the electron acceptor 7,7,8,8-tetracyanoquinodimethane (TCNQ) and the electron donor tetracene using physical vapor transport. The crystal structure was solved by single-crystal X-ray diffraction and the symmetry was found to be triclinic (space group $P\bar{1}$). The 1:1 complex grows by alternating face to face stacking of tetracene and TCNQ molecules. Calculations on the electronic band structure show that the tetracene–TCNQ complex is an indirect band gap semiconductor and provide insight in the conductive properties of tetracene–TCNQ.

1. Introduction

Organic charge-transfer salts are interesting compounds in which the interchain transfer integral can be changed with composition, pressure, and temperature, leading to a delicate balance of interactions that gives rise to a rich variety of physical phenomena. These include charge ordering, spin-Peierls ground state, antiferromagnetism, spin density waves (SDW), metallicity, and superconductivity.¹ In particular, the acene–7,7,8,8-tetracyanoquinodimethane (TCNQ) systems are interesting for electronic applications, as they are semiconductors with a relatively small band gap and a moderate charge-transfer between constituent molecules. Both the value of the energy gap and the charge transfer can be tuned by the nature of the acene molecule and stoichiometry.

In this article, we present the single-crystal growth, crystal structure, and electronic band structure of tetracene–TCNQ complex. The separate constituents were studied by different research groups. Their chemical structure diagrams are presented in Figure 1. Tetracene is a p-type semiconductor with the highest mobility at room temperature, $\mu = 1.3\text{cm}^2/\text{Vs}^2$, reported for transistors fabricated on single crystals and with a SiO_2 gate dielectric chemically treated with octadecyltrichlorosilane (OTS). TCNQ is an n-type semiconductor for which mobilities of $\mu = 1.6\text{cm}^2/\text{Vs}$ were measured for transistors fabricated with “vacuum-gap” dielectric.³

Tetracene and TCNQ, similar to most organic semiconductors, exhibit only unipolar conduction. The absence of ambipolar behavior is a severe limitation for the organic electronic devices for the fabrication of complementary metal oxide semiconductor-like circuits. For many materials, this is not an intrinsic property, but rather a result of a high-energy barrier for either electron or hole injection from the metal electrodes, which is caused by the relatively large band gap of organic semiconductors. Different strategies were proposed to overcome this problem. Most of them involve separate steps to build n-type and p-type transistors. Experiments on thin films have shown that if

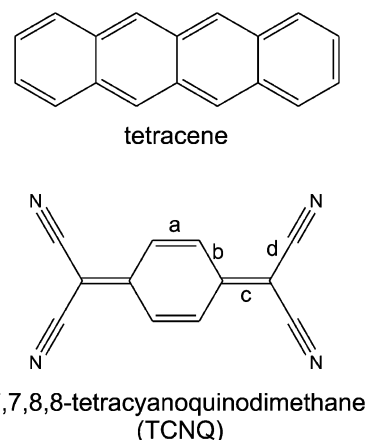


Figure 1. Bond-line formula of tetracene (upper panel) and 7,7,8,8-tetracyanoquinodimethane (lower panel). The size of the bond lengths a , b , c , and d are correlated with the degree of charge transfer between donor and acceptor.

alternative layers of the p-type semiconductor α -hexathienylene (α -6T) and n-type semiconductor C_{60} are evaporated on top of each other, ambipolar field effect transistors can be successfully fabricated.⁴ Solution-processed single layers of heterogeneous blends, consisting of interpenetrating networks of p-type and n-type semiconductors, also showed ambipolar transistor behavior.⁵ However, even if they are attractive for organic electronic devices in thin films (polycrystalline or amorphous), grain boundaries and disorder localize and trap the charge carriers. Here, we propose to incorporate tetracene p-type semiconductor and TCNQ n-type semiconductor in one single-crystal that could combine the electrical properties of the separate constituents and eventually exhibit ambipolar conduction. The study of the conduction in the cocrystal can give a good insight in the interplay between the effect of chemical structure and molecular orientation on the electronic transport.

Electronic structure calculations on several pentacene derivatives have shown that the band structure depends sensitively on the stacking of molecules.¹⁰ A multitude of crystal structures is possible if we combine a donor and acceptor molecule in one crystal structure.

* Corresponding author. E-mail: t.t.m.palstra@rug.nl.

[†] University of Groningen.

[‡] University of Nijmegen.

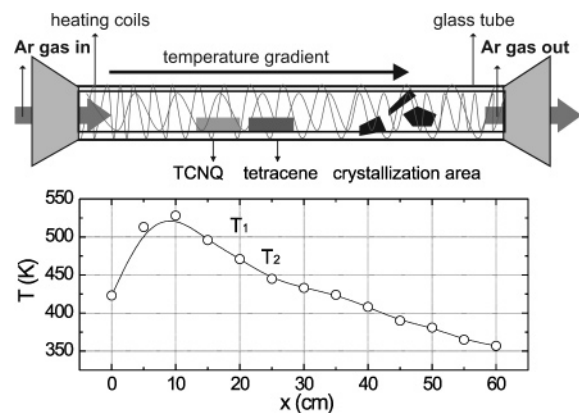


Figure 2. Crystal growth setup. TCNQ and tetracene source materials are placed in the hot part of the tube and the molecules in the gas phase are transported by the argon inert gas to the crystallization region. The temperature profile of the growth tube is shown in the lower panel.

The crystal structures of various charge-transfer salts of TCNQ with different acene donors have been published.^{6–9} Previous attempts to grow similar materials involved the use of solvents. Solvent inclusions are disadvantageous in semiconductor applications. In our method, tetracene–TCNQ cocrystals were grown by physical vapor transport without the use of solvents.

2. Experimental Methods

We have grown cocrystals of tetracene with TCNQ using physical vapor transport in a horizontal glass tube under a stream of argon.¹¹ The gas was obtained from AGA with purity of 99.999%. We removed water and other impurities from the incoming gas stream by an additional filter consisting of active carbon combined with Al_2O_3 and copper. The growth tube setup is presented in Figure 2 (upper panel). The inner tube in which the crystallization takes place has a diameter of 25.8 mm, and the outer, furnace tube has a diameter of 30.1 mm. A temperature gradient was applied by resistive heating of two heater coils around the tubes. The temperature profile is shown in Figure 2 (lower panel). The temperature was controlled using two thermocouples. Prior to growth, the inner tube was cleaned with soap, demineralized water, acetone, and alcohol and was baked out overnight in argon flow to remove water and other solvents. If water is not removed properly, the cyano-nitrile groups of TCNQ can hydrolyze at elevated temperature to amines and eventually to carboxylic acids even in an oxygen-free atmosphere.¹² The presence of hydrolyzation products can be detected in the IR spectrum as distinct peaks at 3300 and 1700 cm^{-1} , characteristic to stretching vibrations in carboxylic acids.

Yellow-colored powder of TCNQ and orange-colored powder of tetracene (Aldrich 99.5%, with no further purification) were placed in separate alumina boats. The boats with the source materials were arranged in the growth tube at positions that correspond to $T_1 = 478$ K (TCNQ) and $T_2 = 459$ K (tetracene), respectively, as shown in Figure 2. The molecules in the vapor phase are transported by the argon gas, and they crystallize in the cold part of the tube. An optimum argon gas flow level is 15 mL/min. This yields needle-shaped crystals formed with typical dimensions of $5 \times 0.1 \times 0.05$ mm. Below a flow level of 10 mL/min, long brittle needles were obtained. Dark brown 1:1 tetracene–TCNQ cocrystals form at temperatures around $T = 423$ K. The crystals are needle-shaped and their dimensions can be controlled by the growth time. Typical growth time is around 3 days.

TABLE 1: Crystal Data, Details of the Structure Determination, Data Collection, and Refinement of Tetracene–TCNQ at 100 K

chemical formula	$\text{C}_{12}\text{H}_4\text{N}_4 \cdot \text{C}_{18}\text{H}_{12}$
formula weight g mol^{-1}	432.48
cell setting	triclinic
space group	$P\bar{1}$
a (\AA)	7.170(2)
b (\AA)	8.599(2)
c (\AA)	8.840(2)
V (\AA^3)	542.9(2)
α	85.638(3) $^\circ$
β	88.905(4) $^\circ$
γ	87.587(4) $^\circ$
Z_{Formula}	1
ρ_{calc} (g cm^{-3})	1.323
data collection method	φ and ω scans
θ range ($^\circ$)	2.84–25.02
unique data	1889
no of refined parameters	186
final agreement factors	
	$wR(F^2) = [\sum w(F_0^2 - F_c^2)^2] / [\sum w(F_0^2)^2]^{1/2}$
	$wR(F^2) = 0.1929$
weighting scheme	$w = 1/[\sigma^2(F_0^2) + (0.1055P)^2 + 0.4694P]$; where $P = \max(F_0^2 + 2F_c^2)/3$
$R(F)$	0.0652
	For F_0 larger than $4.0 \sigma(F_0)$
goodness of fit (S)	1.077
	$S = [\sum [w(F_0^2 - F_c^2)^2] / (n - p)]^{1/2}$
residual electron density ($\text{e}/\text{\AA}^3$)	$\rho_{\text{min}}, -0.23; \rho_{\text{max}}, 0.29$

The single-crystal diffraction experiments were performed on a Bruker SMART APEX CCD diffractometer. A crystal fragment, cut to size to fit in the homogeneous part of the X-ray beam with dimensions of $0.65 \times 0.11 \times 0.05$ mm, was mounted on top of a glass fiber and was aligned on the diffractometer. The diffractometer was equipped with a 4K CCD detector set 60.0 mm from the crystal. The crystal was cooled fast using a Bruker KRYOFLEX and the measurements were performed after the temperature was stabilized. Intensity measurements were performed using graphite monochromated Mo– $K\alpha$ radiation. The structure determination was rather complicated, as the CCD detector revealed multiple reflection spots for each reflection, which showed profiles with anisotropic mosaicity and persistent weak scattering power. Three sets of frames were collected with an exposure time of 30s and an angular step width of 0.3° .

Experimental details about the structure determination at 100 K, data collection, and refinement are summarized in Table 1.

3. Results and Discussion

The unit cell was identified as triclinic, spacegroup $P\bar{1}$. The crystal is close to monoclinic symmetry. However, attempts to assign higher symmetry were not successful.

The crystal structure of tetracene–TCNQ cocrystal is similar to that of complexes consisting of an acene donor (e.g., perylene,⁸ coronene⁹) and TCNQ acceptor. In general, the crystal structure can be considered as a rigid TCNQ structural framework reinforced by intermolecular bonding of CN side groups. The acene is encapsulated in such a framework with slight rotational disorder. Tetracene molecules and TCNQ molecules are stacked face to face in an alternating manner (Figure 3) with a separation which is slightly less than the typical distance for van der Waals interaction (~ 3.4 \AA at 100K). The molecules are not perfectly parallel, rather their molecular planes

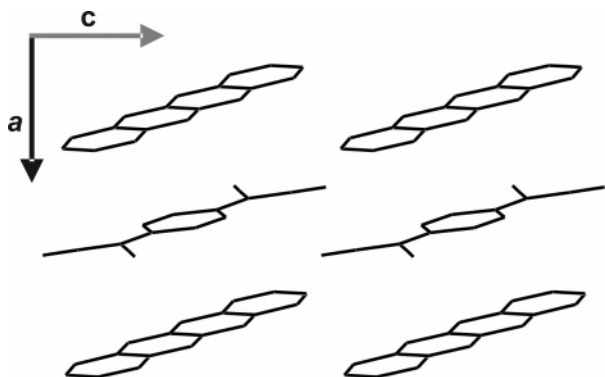


Figure 3. Molecular packing in the tetracene–TCNQ 1:1 cocrystal. The stacking is projected along the *b* crystallographic axis.

TABLE 2: Fractional Atomic Coordinates of the Non-Hydrogen Atoms in Tetracene–TCNQ at 100 K

atom	x	y	z	$U_{eq}(\text{\AA}^2)$
N11	0.6578(3)	0.5095(3)	-0.1797(3)	0.0303(8)
N12	0.6507(3)	0.1603(3)	-0.5102(3)	0.0305(8)
C11	0.5293(3)	0.1529(3)	0.0392(3)	0.0199(8)
C12	0.5503(3)	0.1128(3)	-0.1169(3)	0.0196(8)
C13	0.5176(3)	-0.0445(3)	-0.1495(3)	0.0212(8)
C14	0.6007(3)	0.2232(3)	-0.2298(3)	0.0187(8)
C15	0.6320(4)	0.3815(3)	-0.2010(3)	0.0225(8)
C16	0.6272(4)	0.1869(3)	-0.3853(3)	0.0229(8)
C21	0.1802(4)	0.3590(4)	-0.4342(4)	0.0435(11)
C22	0.1326(4)	0.2082(4)	-0.4009(3)	0.0335(10)
C23	0.0868(3)	0.1522(3)	-0.2479(3)	0.0243(8)
C24	0.0379(4)	-0.0007(3)	-0.2092(3)	0.0234(8)
C25	-0.0040(3)	-0.0540(3)	-0.0585(3)	0.0202(8)
C26	-0.0527(4)	-0.2086(3)	-0.0188(3)	0.0235(8)
C27	0.0945(3)	0.2597(3)	-0.1308(3)	0.0241(8)
C28	0.1473(4)	0.4164(3)	-0.1711(4)	0.0325(10)
C29	0.1880(4)	0.4640(4)	-0.3184(4)	0.0390(11)

make an angle of 1.7° in the *ab* plane and an angle of 1.4° in the *ac* plane, respectively.

The alternative stacking of the two different constituent molecules in the complex occurs along the *a* crystallographic axis, which is also the primary axis of crystal growth. The long axes of the planar donor and acceptor molecules make a small angle of 3.5° . The one-dimensional character of the π overlap is expected to cause anisotropy in morphology and electronic properties.

The structure was solved by direct methods, using the program SIR-97.¹³ The positional and anisotropic displacement parameters for the non-hydrogen atoms were refined. A subsequent difference Fourier synthesis resulted in the location of all the hydrogen atoms, which coordinates, and isotropic displacement parameters were refined. The fractional coordinates of all the atoms in the tetracene–TCNQ cocrystals are presented in Table 2.

As derived from the single-crystal X-ray diffraction experiments, the stacking distance between the alternative molecules in the crystal is relatively small ($\sim 3.4 \text{ \AA}$ at 100K).

The degree of charge transfer can be calculated from the geometry of the TCNQ molecule, determined from diffraction experiments.¹⁴ The neutral TCNQ molecule presents typical values for the bond lengths *a*, *b*, *c*, *d* presented in Figure 1. As it gets charged in the cocrystal due to the presence of the electron donor tetracene, the bond length *a* and *c* in Figure 1 dilate, whereas bond lengths *b* and *d* tend to shrink. The differences *b*–*c* and *c*–*d* follow the degree of charge transfer with null values in the case of $z = -1$, and $b-c = 0.069$ and $c-d = -0.062$ for the neutral molecule. The values for the bond

TABLE 3: Comparison between Calculated and Measured Bond Distances

atom1–atom2	X-ray diffraction	calculated
N11–C15	1.154(4)	1.169
N12–C16	1.152(4)	1.169
C11–C12	1.451(4)	1.432
C12–C13	1.434(4)	1.436
C12–C14	1.378(4)	1.405
C14–C15	1.431(4)	1.415
C14–C16	1.440(4)	1.414
C11–H11	0.91(3)	1.089
C13–H13	0.95(3)	1.089
C21–C22	1.364(5)	1.374
C22–C23	1.438(4)	1.424
C23–C24	1.391(4)	1.400
C24–C25	1.407(4)	1.404
C25–C26	1.406(4)	1.410
C27–C28	1.432(4)	1.428
C28–C29	1.365(5)	1.371
C21–H21	1.05(4)	1.088
C22–H22	1.02(3)	1.089
C24–H24	0.96(3)	1.090
C26–H26	1.03(3)	1.090
C28–H28	1.13(4)	1.088
C29–H29	0.99(4)	1.089

lengths of the partially charged TCNQ molecule in the tetracene–TCNQ complex at 100 K are

$$\begin{aligned}
 a &= 1.345 \text{ \AA} \\
 b &= 1.451 \text{ \AA} \\
 c &= 1.378 \text{ \AA} \\
 d &= 1.431 \text{ \AA}
 \end{aligned}
 \quad (1)$$

The calculations derived from the X-ray diffraction experiments show that the 1:1 tetracene–TCNQ complex present a limited charge transfer, $z \cong 0.1$. This value is significantly lower than for typical organic charge-transfer complexes (e.g., tetrathiafulvalene–TCNQ^{1,16}), but similar to what is reported for other acene–TCNQ systems.⁹ Strictly speaking, acene–TCNQ complexes should in this respect not be called charge-transfer salts.

The band structure of tetracene–TCNQ complex was calculated using ab initio simulation package VASP (Vienna ab initio Simulation Package)^{17–22} based on density functional theory (DFT) in the generalized gradient approximation (GGA). This is a full potential method that does not make any approximation to the shape of the potential. This is important because organic semiconductors usually possess lower symmetry as compared to traditional solids. The method based on DFT implies that band gaps are usually underestimated; however, the band topologies are accurately described. The electronic band structure calculation methods were successfully applied to a number of organic semiconductor materials.^{10,24–26}

Prior to the band structure calculations, the atomic positions obtained from X-ray diffraction measurement were optimized with a force tolerance of 10 meV/\AA . Some of the interatomic distances are listed in Table 3.

In Figure 5 the band structure along three directions $X(a^*)$, $Y(b^*)$ and $Z(c^*)$ is shown. On the basis of the band structure, tetracene–TCNQ is found to be an indirect band gap semiconductor with a valence band maximum at *Y*. We are able to predict the conductive properties of tetracene–TCNQ from the relative widths of the conductive and valence bands.

The electron conductivity will be the highest in *X* direction while the highest hole conductivity is expected in *Y* direction, as follows from the relative widths of the valence and conduction band. However, we have not yet obtained reproducible results for ambipolar conduction in tetracene–TCNQ. The analysis of

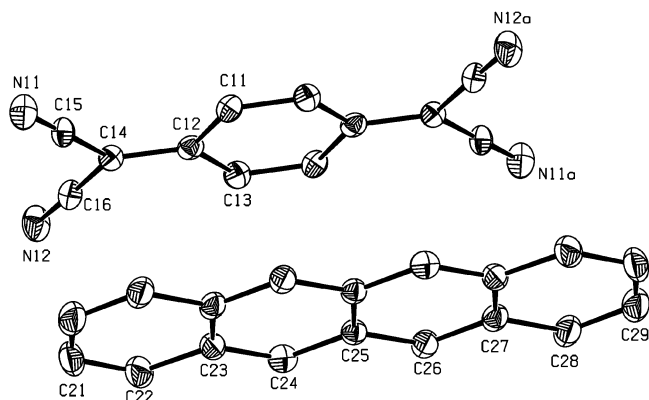


Figure 4. Perspective ORTEP¹⁵ drawing of the tetracene–TCNQ complex, illustrating the conformation and the adopted labeling scheme for the non-hydrogen atoms. Displacement ellipsoids for non-H atoms are represented at the 50% probability level.

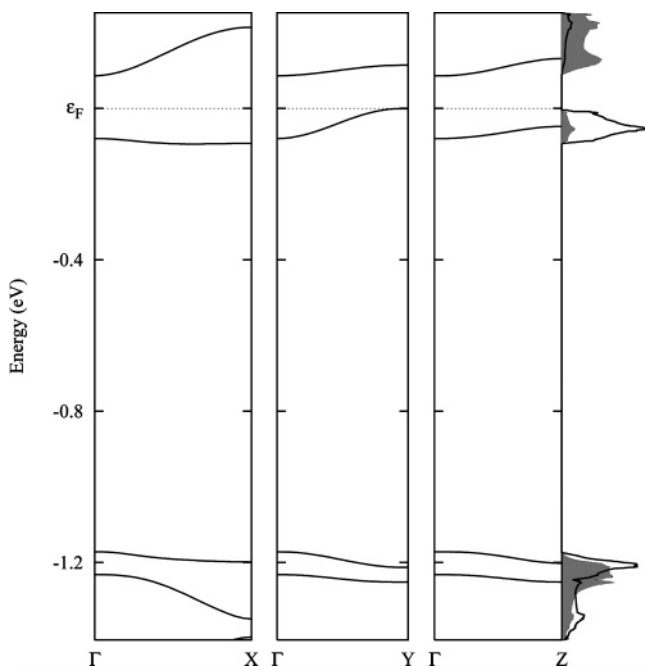


Figure 5. Electronic structure of the valence and conduction bands of tetracene–TCNQ along $X = (a^*/2)$, $Y = (b^*/2)$ and $Z = (c^*/2)$ direction. The Fermi energy was chosen on top of the valence band. X is the molecular stacking direction. The density of states in arbitrary units per molecule per unit cell (gray area for TCNQ and white area for tetracene) is shown on the right-hand side.

the partial density of states shows that the tetracene moiety contributes predominantly to the valence band states, whereas the states in the conduction band are dominated by the TCNQ molecule. Because of the cofacial arrangement of the tetracene with respect to TCNQ molecules within the crystal of tetracene–TCNQ, the largest π -orbital overlap and hence the interaction is expected to be in the stacking (i.e., X direction). One can establish by inspection of the relative band dispersions along the stacking direction, as shown in Figure 5, that the LUMO interacts strongest with the HOMO–2 and very weakly with the HOMO band. A more detailed comparative and systematic study of tetracene–TCNQ and some other similar TCNQ complexes will be presented elsewhere.²³

4. Conclusions

We have grown tetracene–TCNQ cocrystals by physical vapor transport in an inert atmosphere. The crystals are formed

by alternation of the donor and acceptor molecule along the a -crystallographic axis, the primary axis of crystal growth, and the charge transfer between the two constituent molecules is 0.1. The electronic band structure calculations show that tetracene–TCNQ complex is an indirect band gap semiconductor with a valence band maximum at Y .

Acknowledgment. This work was supported by the MSC^{plus} (Materials Science Centre) and is part of the research programme of the Stichting voor Fundamenteel Onderzoek der Materie (FOM) with financial support from the Nederlandse Organisatie voor Wetenschappelijk Onderzoek (NWO).

References and Notes

- J rome, D. *Chem. Rev.* **2004**, *104*, 5565.
- Goldmann, C.; Haas, S.; Krellner, C.; Pernstich, K. P.; Gundlach, D. J.; Batlogg, B. *J. Appl. Phys.* **2004**, *96*, 2080.
- Menard, E.; Podzorov, V.; Hur, S.-H.; Gaur, A.; Gershenson, M. E.; Rogers, J. A. *Adv. Mat.* **2004**, *16*, 2097.
- Dodabalapur, A.; Katz, H. E.; Torsi, L.; Haddon, R. C. *Appl. Phys. Lett.* **1996**, *68*, 1108.
- Meijer, E. J.; De, Leeuw, D. M.; Setayesh, S.; van Veenendaal, E.; Huisman, B. H.; Blom, P. W. M.; Hummelen, J. C.; Scherf, U.; Klapwijk, T. M. *Nat. Mat.* **2003**, *2*, 678.
- Williams, R. M.; Wallwork, S. C. *Acta Crystallogr. B* **1968**, *24*, 168.
- Tickle, I. J.; Prout, C. K. *J. Chem. Soc., Perkin Trans.* **1973**, *2*, 727.
- Tickle, I. J.; Prout, C. K. *J. Chem. Soc., Perkin Trans.* **1973**, *2*, 720.
- Chi, X.; Besnard, C.; Thorsm lle, V. K.; Butko, V. Y.; Taylor, A. J.; Siegrist, T.; Ramirez, A. P. *Chem. Mater.* **2004**, *16*, 5751.
- Haddon, R. C.; Chi, X.; Itkis, M. E.; Anthony, J. E.; Eaton, D. L.; Siegrist, T.; Mattheus, C. C.; Palstra, T. T. M. *J. Phys. Chem. B* **2002**, *106*, 8288.
- Laudise, R. A.; Kloc, C.; Simpkins, P.; Siegrist, T. *J. Cryst. Growth* **1998**, *187*, 449.
- Vollhardt, K. P. C.; Schore, N. E. *Organic Chemistry: Structure and Function*, 3rd edition; Freeman: New York, 1998.
- (a) Altomare, A.; Burla, M. C.; Camalli, M.; Cascarano, G. L.; Giacovazzo, C.; Guagliardi, A.; Moliterni, A. G. G.; Polidori, G.; Spagna, R. *J. Appl. Cryst.* **1999**, *32*, 115. (b) SIR-97 is a package for crystal structure solution by direct methods and refinement developed by University of Bari, University of Perugia, and University of Roma, Italy
- Flandrois, S.; Chasseau, D. *Acta Crystallogr. B* **1977**, *33*, 2744.
- Spek, A. L. *J. Appl. Crystallogr.* **2003**, *36*, 7.
- Ferraris, J.; Cowan, D. O.; Walatka, V.; Perlstein, J. H. *J. Am. Chem. Soc.* **1973**, *95*, 948.
- Kresse, G.; Hafner, J. *Phys. Rev. B* **1993**, *47*, 558.
- Kresse, G.; Hafner, J. *Phys. Rev. B* **1994**, *49*, 14251.
- Kresse, G.; Furthm ller, J. *Phys. Rev. B* **1996**, *54*, 11169.
- Kresse, G.; Furthm ller, J. *Comput. Mater. Sci.* **1996**, *6*, 15.
- Kresse, G.; Joubert, D. *Phys. Rev. B* **1998**, *59*, 1758.
- Bl chl, P. E. *J. Phys. Rev. B* **1994**, *50*, 17953.
- Shokaryev, I. et al. Unpublished work.
- Brocks, G. *Phys. Rev. B* **1997**, *55*, 6816.
- Siegrist, T.; Kloc, C.; Laudise, R. A.; Katz, H. E.; Haddon, R. C. *Adv. Mater.* **1998**, *10*, 379.
- Troisi, A.; Orlandi, G. *J. Phys. Chem. B* **2005**, *109*, 1849.